

DESIGN METHODS FOR COMPOSITE REINFORCED METALLIC BEAMS

Dag Linghoff¹ and Alann André²

¹Chalmers University of Technology, 412 96 Göteborg, Sweden, dag.linghoff@chalmers.se

²SWEREA SICOMP AB, Box 104, 431 22 Mölndal, Sweden, alann.andre@swerea.se

ABSTRACT

A new method for repair or strengthening of metallic structures has been developed and investigated during the recent years. The traditional way of upgrading metallic beam elements have been by use of additional metallic plates, which have been either bolted or welded to the existing substrate. The new method involves use of advanced composite plates, commonly made of unidirectional carbon fibre reinforced polymers (CFRP). The CFRP plates are adhesively bonded to the metallic beam to reduce the stresses in the tension area of the metallic section. Today, there are no established codes or standards for structural design of externally reinforced metallic beams in civil engineering. However, two different approaches have been recommended in different guidelines [1] and [2] with respect to design of the adhesive joint, but there is a shortage in evaluation of these two methods. Present paper gives a briefly description of a conducted numerical evaluation study.

1. INTRODUCTION

The present study is limited to comprise the design of the adhesive joint due to debonding near the end of the CFRP plate. Irrespective of which load combinations acting on the beam causing a bending moment, a concentration of interfacial shear and peeling stresses will appear in the bond line near the end of the CFRP. These stresses have to be carried by the resistance of the compositely acting materials, either the adherents or the adhesive. The general design criterion that has to be fulfilled is that the resistance of the adhesive joint is at least equal or higher than the effect of actions.

For metallic beams reinforced with adhesively bonded CFRP plates on the tension side, two different approaches are developed for predicting the capacity of the adhesive joint, namely the stress based method and the fracture mechanic based method.

The design philosophy in the stress based method is that the interfacial shear and peeling stresses, which appear in the bond line due to transfer of forces between the metallic beam and the CFRP plate, are converted to a principle stress. This principle stress due to the load effect is then compared with a principle stress obtained from a resistance investigation of a similar joint. The available solutions for calculate the interfacial stresses are all based on elastic theory. Thus, the solution will not take any redistribution of stresses into account. Neither can the effect of bond defects be considered. Instead, it is assumed that the magnitude of the peak stress in the adhesive layer will govern the failure of the adhesive joint, and it is assumed that the peak shear and peeling stresses in the adhesive joint appear at the same location. Investigations (e.g. [3], [4]) pronounce that the peel stress is particularly damaging because the unidirectional CFRP plate possesses less resistance to peel stress than any other mode of loading. Therefore, it is uncertain if an elastic design criteria based on the principle stress in the adhesive layer is representative in the design of a CFRP reinforced metallic beam.

The linear elastic fracture mechanic is an ultimate analysis and two different approaches are available for design of adhesive joint in civil engineering. One is the energy release rate approach and the other is the stress intensity factor approach. In existing guidelines, for design of adhesive joints in CFRP reinforced metallic beams, an energy based method founded on the energy release rate approach is considered. The energy release rate approach considers the energy released during the propagation of the crack along the adhesive joint, and the method inherently takes account to the existence of stress discontinuities. The design philosophy is that the fracture energy release rate (G), which also can be denoted crack extension force or crack deriving force, during propagation of the crack is obtained and compared with the critical energy release rate (G_C) and the criterion is that $G \leq G_C$. Mode I failure is normally assumed to dominate failure of composite adhesive – CFRP joints. Even if Mode I failure is an assumed governing failure mode, fracture energies obtained from this mode may not lead to conservative designs for composite adhesive joints, see [5]. Therefore, it is advisable to carry out a characterisation for a range of mode mixities for a thorough understanding of how a given adhesive system may perform during fracture events. Nevertheless, the effect of mode mixity on measured fracture energy seems still to be poorly understood, especially in practical engineering adhesive joints. Another major problem with the energy based method is to predict an initial crack length.

From a review of available design approaches, it is noticeable that there is lack of knowledge in the field of analysing and design of adhesively bonded elements in structural engineering, and this is reflected by the use of high partial factors. Additionally, there is no general agreement of which design method that is the most suitable to obtain a sufficiently good design. In the present investigation the available design methods, which are described above, have been evaluated and a fracture mechanic model, based on cohesive elements, has been developed. One of the major aims with this investigation was to obtain information about how well the available design methods represent the real behaviour and failure of an externally CFRP reinforced structural element loaded in bending. For evaluation of the existing proposed design methods finite element (FE) and analytical analyses have been carried out. Investigation of the results from these tests in combination with the results from the fracture mechanic based FE analyses could predict the locus of the failure. Additionally, the results show either if it is the peak stresses that governs the failure or if the failure appear when a certain amount of energy in the adhesive joint is consumed. One of the advances with the developed fracture mechanic model is that no initial crack length has to be predicted. A full-scale beam test and adhesive joint tests are ongoing within the frame of the project to verify the analytical and numerical results and to provide material properties.

2. MODEL SET-UP

The focus is put on Carbon Fiber Reinforced Polymer (CFRP) reinforced steel I beam (IPE 200). The geometry and dimensions of the beam are shown in Figure 1 and Table 1. In order to capture debonding failure of the adhesive layer before steel yielding, a relatively short length of CFRP laminate was used.

Table 1: Geometry of the experimental set-up [mm].

L_{beam}	L_{CFRP}	b_f	t_f	h_w	t_w	b	h_{adh}	h_{CFRP}
1800	500	100	8.5	183	5.6	30	2	2.4

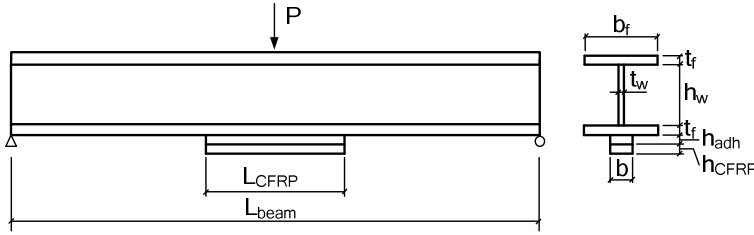


Figure 1: Experimental set-up – Steel I beam reinforced CFRP plate.

In order to characterize the debonding and delamination behaviour of the adhesive and the CFRP respectively, Double Cantilever Beam (DCB) tests and End Notched Flexural (ENF) tests will be performed, see Figure 2. The results give respectively information (strength, cohesive law, fracture energy, crack opening) in mode I and II for the two systems.

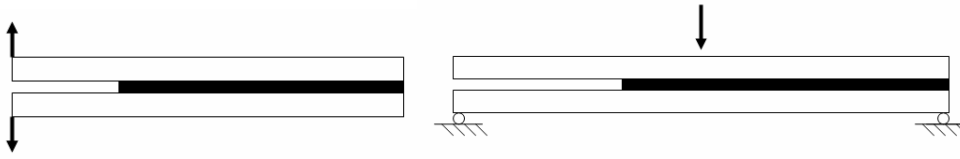


Figure 2: Experimental set-up – DCB (left) and ENF (right).

2.2 Analytical model for interfacial stresses

There are closed-form solutions available for calculation of the interfacial shear and peeling stresses in the adhesive layer. A general assumption for all solutions is that the bond line is subjected to interfacial shear and peeling stresses, which are constant through the thickness of the adhesive layer. The characteristics for the stress based methods are that the analysis of the bond line is based on elastic theory and that strain varies linearly across the adhesive thickness. In the solutions it is also assumed that the peak values for the interfacial stress appear at the same location, namely at the outermost end of the bond line. One of the most well known closed-form solution, used for metallic beams with adhesively bonded CFRP plates, is the one developed by Smith and Teng [6]. The solution is based on the force equilibrium of a strengthened section and use of shear compatibility.

In the proposed design guide lines ([1], [2]) a failure criterion is established where the principle stress based on the calculated interfacial shear (τ) and peeling (σ) stresses in the bond line are compared with a principle stress ($\bar{\sigma}$) obtained from analysis of a lap-joint test. The criterion is given in Equation 1.

$$\sigma_I = \frac{\sigma}{2} + \sqrt{\left(\frac{\sigma}{2}\right)^2 + \tau^2} \leq \bar{\sigma} \quad (1)$$

In this study the analytical solution by Smith and Teng (2001) was used to investigate of how well the results from numerical analyses and analytical solutions agree. In the analytical model there is no possibility to model the CFRP as an orthotropic material. Instead, the Young's modulus in the fibre direction of the laminate was used.

3. FE MODELS

Two different FE models have been used for the analysis of the adhesive layer. The commercial FE software Abaqus [8] was used. Each model is described in the

following parts and comparisons of the results from the models are given in a separate section.

The material models for CFRP, steel and adhesive have been reported in Table 2. The adhesive material model is defining as a linear elastic material in the 2D-stress model while the 3D-cohesive model considers the fracture toughness in mode I and II. The fracture toughness of the adhesive are estimated and will be verified by DCB and ENF results.

Table 2: Material models

CFRP	E₁₁ (GPa)	E₂₂ (GPa)	E₃₃ (GPa)	ν₁₂	ν₁₃	ν₂₃	G₁₂ (GPa)	G₁₃ (GPa)	G₂₃ (GPa)
	210	10	10	0.3	0.3	0.5	5	5	3
Steel	E (GPa)	ν							
	210	0.3							
Adhesive 2D-stress	E (GPa)	ν							
	4.5	0.3							
Adhesive 3D-cohesive	E (GPa)	ν	σ_{max} (MPa)	τ_{max} (MPa)	G_{Ic} (J/m ²)	G_{IIc} (J/m ²)			
	4.5	0.3	25	25	1000	3000			

Perfect bonds are assumed at the steel - adhesive and adhesive – CFRP interface, which implies that failure is assumed to initiate in the adhesive layer. Only failure mode B (Figure 3) is considered in the present investigation.

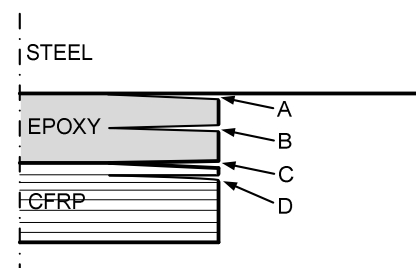


Figure 3: Different failure modes in steel beams strengthened with adhesively bonded CFRP-laminates; A) Interfacial failure between steel and adhesive, B) Cohesive failure, C) Interfacial failure between adhesive and CFRP and D) Delamination of CFRP laminate.

3.1 Stress based models

According to proposed design methods the interfacial stresses is calculated in the mid-thickness of the adhesive layer. A FE-model was created to generate the interfacial shear and peeling stresses on that location along the bond line. The FE model used for this analysis was created by using 3D shell elements with 8-nodes (S8R), where this element type was assigned to all parts in the model. The shortcoming with using shell elements instead of solid elements is that the interfacial stresses along the width of the adhesive layer can not be extracted. Instead, a uniform stress distribution is obtained and no effect of flange curling or shear lag is considered. For wide-flanged I-section beams the effect of flange curling can have an affect on the interfacial stresses, where the stresses will be more concentrated to the region near the web of the cross-section, [7]. By neglecting these effects the design may be non-conservative.

By use of the longitudinal symmetry, only one half of the beam was modelled and a symmetry boundary condition was used in the mid-span. The support was modelled with rigid links acting over a distance of 50 mm and connected to a reference point which was allowed to translate in the longitudinal direction and rotate around an axle perpendicular to the extension of the beam. The point load was applied as an edge load over a distance of 50 mm. The load and boundary conditions are illustrated in Figure 4.

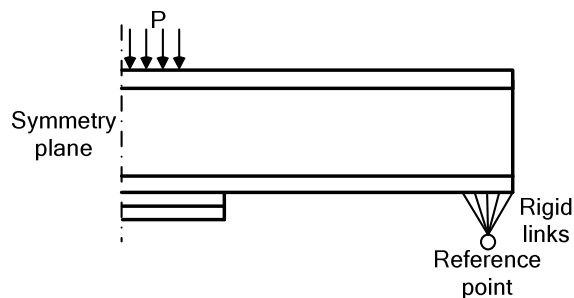


Figure 4: Illustration of the load and boundary conditions

The mesh used for the beam in the model varied in size and geometry. A small region near the end of the adhesive layer, 20 mm long, a dense mesh with quadratic was used. The adhesive layer was 2 mm thick and was meshed with 8 elements over the thickness (Figure 5). Thus, the element size was 0.25 mm x 0.5 mm. A convergence study showed that this element size gave acceptable results.

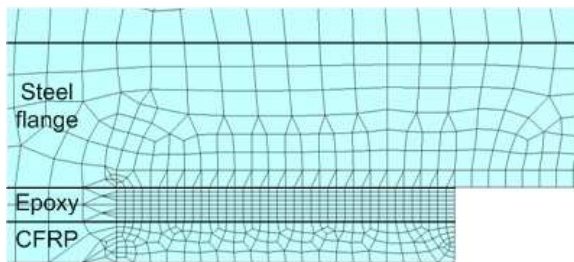


Figure 5: The geometry of the mesh at the end of the adhesive layer.

3.2 Stress and energy based model with cohesive elements

The debonding or delamination processes of composite material occur in two main steps: the damage initiation and the damage propagation.

Under bending, the adhesive bonding the CFRP to the I-beam is mainly subjected to mode I and mode II opening due to peel and shear stresses. The cohesive law for each mode captures the linear elastic and softening behaviour before fracture, and can be obtained by performing Double Cantilever Beam tests and End Notched Flexural beam tests. In that part, the focus will be on the use of cohesive elements together with a traction separation law (TSL) to model the adhesive.

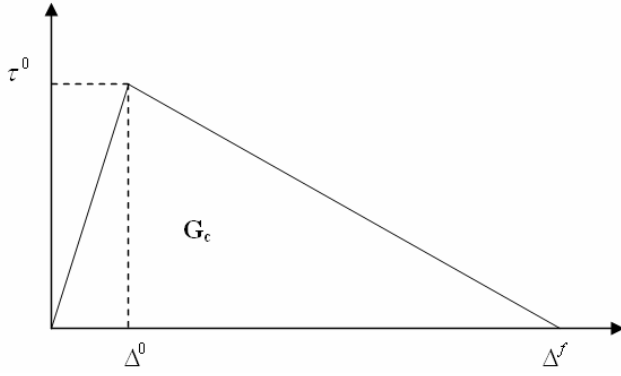


Figure 6: Bilinear traction separation law.

Cohesive elements in Abaqus [8] can be defined by a linear elastic response, a strength criteria and a damage evolution law based on energies. The damage initiation starts when a quadratic criterion is fulfilled. The strength of the adhesive in the normal and shear directions are used as input data.

$$\left(\frac{\sigma_{33}}{\hat{\sigma}_{33}}\right)^2 + \left(\frac{\tau_{13}}{\hat{\tau}_{13}}\right)^2 + \left(\frac{\tau_{23}}{\hat{\tau}_{23}}\right)^2 = 1 \quad (2)$$

The damage evolution is governed by a damage parameter D which describes the rate of stiffness softening after damage initiation.

The adhesive layer is most likely mixed mode loaded, i.e. we have a contribution of mode I and II in the failure process. The damage propagation is studied in term of energy release rate and fracture toughness. In order to accurately predict the mode mixity of the epoxy under loading [9], the Benzeggagh-Kenane criteria BK is used [10].

$$G_{Ic} + (G_{IIc} - G_{Ic}) \left(\frac{\beta}{1 + 2\beta^2 - 2\beta} \right)^\eta = G_{mc} \quad (3)$$

where G_{Ic} and G_{IIc} are the fracture toughness in mode I and II respectively. The exponent η is chosen to 1.45. β is the parameter determining the mixed mode ratio based on the current values of the peel and shear opening in the TSL for mode I and II respectively.

$$\beta = \frac{\Delta_{shear}}{\Delta_{peel} + \Delta_{shear}} \quad (4)$$

The fracture toughness function of the mixed mode ratio is plotted in Figure 7. It was observed from the finite element analysis that the mixed mode ratio was varying depending on the position along the bond line.

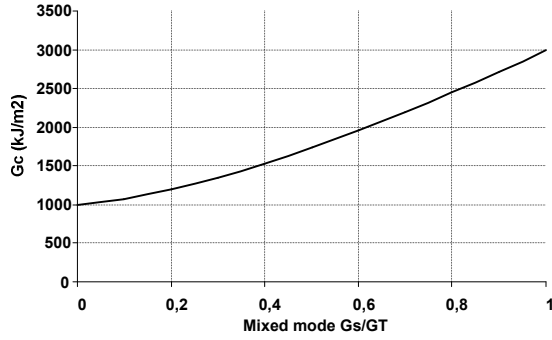


Figure 7: Fracture toughness function of mixed mode ratio

The softening part of the traction separation curve is defined as linear by a damage parameter D . The maximum displacement at failure can be related to the parameters of the BK criterion:

$$D = \frac{\Delta^f \cdot (\Delta^{\max} - \Delta^0)}{\Delta^{\max} \cdot (\Delta^f - \Delta^0)} \quad \text{with} \quad \Delta^f = \frac{2G_{mc}}{\tau^0} \quad (5)$$

The 3D CFRP reinforced I beam was modelled using transversal and longitudinal symmetry, i.e. one fourth of the beam was considered. Solid brick elements with 8 nodes (C3D8) were used for the steel beam and the CFRP. The adhesive was modelled with cohesive elements (COH3D8). A FE mesh of the model is shown in Figure 8. The cohesive elements were connected to the surrounding 3D elements (steel and CFRP) through surface based tie constraint. A very fine mesh was used in the reinforced area. The cohesive element size along the span direction was 0.5 mm. Only one element was used through the adhesive thickness. In the reinforced area, the element size in the steel and in the CFRP was 0.5 mm along the span direction.

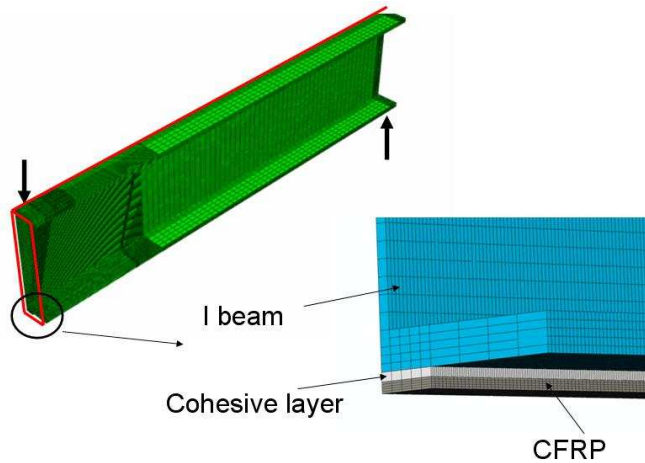


Figure 8: FE mesh of a beam model.

The beam was loaded in displacement control and the load was recorded at the support.

4. RESULTS AND DISCUSSION

To verify the comparability of the FE models and the theoretical model, the load displacement curves are plotted together (3D-cohesive model, 2D-stress model and Smith and Teng [6] analytical model), see Figure 9. The differences between the slopes of the three curves are considered small enough to be able to compare the results of the

three models. It is interesting to point out that the load-displacement curves of the 2D-stress model and the analytical model are almost confounded. The 3D-cohesive model presents a slightly lower slope. The deflection at 120 kN is about 4.5 mm.

For the stress-based analyses, the interfacial shear and peeling stresses and the principal stresses (σ_1) were extracted in the mid-thickness of the epoxy layer. The principal stress was calculated according to Equation (1) above. The stresses from the 2D-stress model were extracted at an increment where the peak value of the principal stresses was equal to 25 MPa, which means that the ultimate strength of the epoxy is theoretically reached. The 2D-stress model gave a failure load equal to 107 kN. From the closed-form solution by Smith and Teng [6] the failure load was calculated to be 116 kN.

A comparison of the interfacial stress distribution between the 2D-stress FE-model and the closed-form analytical solution along the adhesive layer are given in Figure 9. In the plot a small disturbance of the stress distribution is visible at 20 mm from the end, and this is due to a change in the mesh size and has no physically meaning.

The shear and peeling stress components from the 2D-stress analysis and analytical solution were not in a good agreement. The shear stress from the analytical solution was 20 MPa and appeared at the end of the bond line, while for the 2D-stress analysis the maximum shear stress was 17.4 MPa at a distance of 1.5 mm from the end of the bond line. The difference in peeling stresses was larger, 15.9 against 9.9 MPa from the analytical solution.

When the principal stress distribution along the bond line is studied for all three models, a good agreement can be seen. At the level of maximum principal stress the non linear fracture mechanic (NLFM) analysis showed that degradation of the adhesive started at the outermost end of the bond line and propagated in the inward direction along the adhesive.

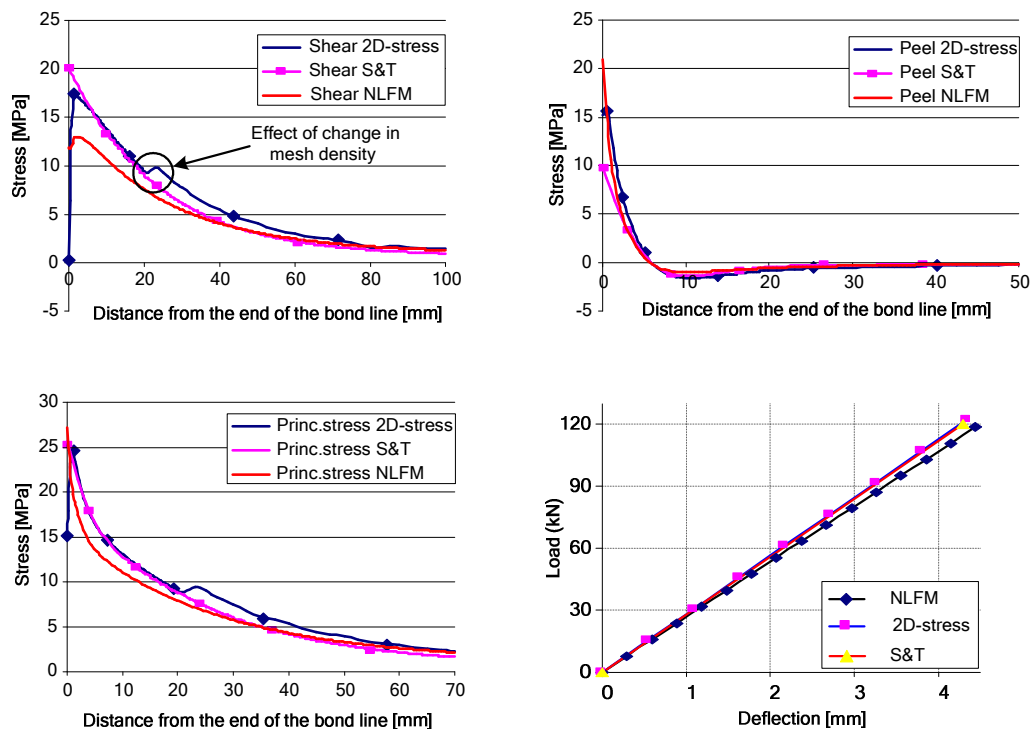


Figure 9: Peel, shear and principal stress in the adhesive layer.

The quadratic stress criterion evolution under loading was studied. The contour plots representing the value of the criterion (varying between 0 and 1, 1 indicating that the criterion is fulfilled) are shown in Figure 10. At 103 kN, the stress criterion in the first elements at the end of the bond line is equal to 0.97. This value indicates that the stiffness degradation process will soon start.

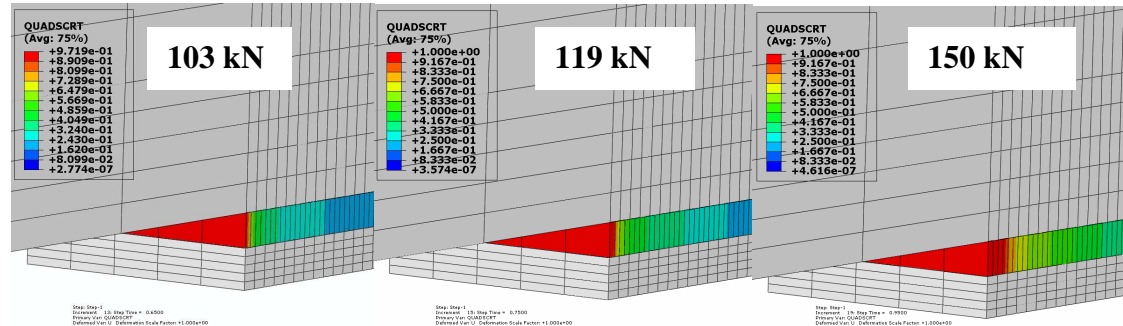


Figure 10: Quadratic stress criteria evolution under loading.

Figure 11 shows the plot of the damage criteria and the stiffness degradation in the element closest to the end of the bond line under loading. At 150 kN, the steel is yielding ($\sigma_y = 355$ MPa). The steel material model does not consider plasticity and the FE-model was therefore only studied up to 150 kN.

At 105 kN, the element at the end of the bond line fulfil the quadratic stress criteria and the damage evolution (stiffness degradation) process starts. When the load equals 150 kN, the stiffness degradation reach a value close to 40%.

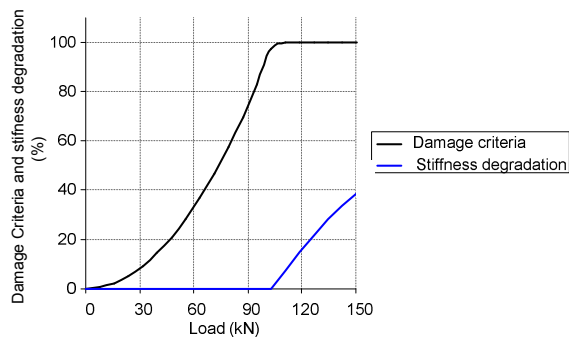


Figure 11: Damage initiation criteria and stiffness degradation evolution under loading in the bond end element.

5. CONCLUSIONS

A steel I-beam reinforced with CFRP has been studied analytically and with two FE-models, one stress-based and one energy-based. The results have been compared in order to evaluate the magnitude of the applied load causing failure in the adhesive layer. From these analyses following conclusion can be drawn:

- All models give a different picture of the shear and peeling stress distribution at the end of the adhesive. The assumption that maximum shear and peel stress occur in the same section at the end of the bond line [6] is not confirmed by the FE-models. Ongoing experiments with speckle pattern analyses of the adhesive will provide better knowledge about the stress field.

- However, even if there were discrepancies between the two interfacial components from the analytical solution, 2D-stress and NLFM analyses the same principal stress was reached for a certain load level, which imply that the failure criterion of the adhesive was reached at almost the same load for the three analyses.

Further studies of the adhesive layer will consider all possible failure modes presented above. For this purpose a FE-model using cohesive layers at both interfaces steel/adhesive and CFRP/adhesive together with solid element in the remaining adhesive thickness will be conducted.

ACKNOWLEDGEMENTS

Vinnovas KSP-programme - Project: *Demontering av limförband* is gratefully acknowledged for sponsoring this research work.

REFERENCES

1. Cadei, J.M., Stratford, T.J. Hollaway, T.C. and Duckett, W.G. "Strengthening metallic structures using externally bonded fibre-reinforced polymers". CIRIA, Publication C595, 2004.
2. Schnerch, D., Dawood, M. and Rizkalla, S. "Strengthening of steel-concrete composite bridges with high modulus carbon fiber reinforced polymer (CFRP) strips". Technical report No. IS-06-02. North Carolina State University, 2007.
3. Hutchinson, A.R. and Hurley, S.A. "Transfer of adhesively technology – Feasibility study". Project report 84, CIRIA. London, 2001.
4. Keller, T. and Vallée, T. "Adhesively bonded lap-joints from pultruded GFRP profiles – Part II: joint strength prediction". Composites Part B, vol. 36, 2004.
5. Adams, R.D. (editor). "Adhesive bonding – Science, technology and applications". Woodhead Publishing Limited, Abington Hall, Cambridge, England. ISBN 1-8557-3741-8. 2005.
6. Smith, S.T and Teng, J.G. "Interfacial stresses in plated beams". Engineering Structures, vol. 23, pp. 857-871, 2001.
7. Linghoff, D., Al-Emrani, M. and Kliger, R. "Performance of steel beams strengthened with CFRP laminate – Part 1 - Laboratory test". Submitted to Composites Part B: Engineering 2007.
8. ABAQUS (2007). "V6.7, © ABAQUS, Inc."
9. Camanho, P. P., and C. G. Davila, "Mixed-Mode Decohesion Finite Elements for the Simulation of Delamination in Composite Materials," NASA/TM-2002–211737, pp. 1–37, 2002.
10. Benzeggagh, M. L., and M. Kenane, "Measurement of Mixed-Mode Delamination Fracture Toughness of Unidirectional Glass/Epoxy Composites with Mixed-Mode Bending Apparatus," Composites Science and Technology, vol. 56, pp. 439–449, 1996
11. Reeder, J.R., "An Evaluation of Mixed-Mode Delamination Failure Criteria", 1992, NASA TM 104210.